LETTER

Effect of the Incorporation of a Low-Band-Gap Small Molecule in a Conjugated Vinylene Copolymer: PCBM Blend for Organic Photovoltaic Devices

P. Suresh,[†] P. Balraju,[†] G. D. Sharma,*[,†] John A. Mikroyannidis,*[,‡] and Minas M. Stylianakis[‡]

Molecular Electronic and Optoelectronic Device Laboratory, Physics Department, JNV University, Jodhpur 342005, India, and Chemical Technology Laboratory, Department of Chemistry, University of Patras, GR-26500 Patras, Greece

ABSTRACT The effect of the incorporation of a low-band-gap small-molecule BTD-TNP on the photovoltaic properties of vinylene copolymer P:PCBM bulk heterojunction solar cells has been investigated. The introduction of this small molecule increases both the short-circuit photocurrent and the overall power conversion efficiency of the photovoltaic device. The incident photon-to-current efficiency (IPCE) of the device based on P:PCBM:BTD-TNP shows two distinct bands, which correspond to the absorption bands of P:PCBM and BTD-TNP. Furthermore, it was found that the IPCE of the device has also been enhanced even at the wavelengths corresponding to the absorption band of P:PCBM, when the thermally annealed blend was used in the device. This indicates that the excitons that are generated in copolymer P are dissociated into charge carriers more effectively in the presence of the BTD-TNP small molecule at the copolymer P:PCBM interface by energy transfer from P to the small molecule. Therefore, we conclude that the BTD-TNP small molecule acts as light-harvesting photosensitizer and also provides a path for the generated exciton in copolymer P toward the P:PCBM interface for efficient charge separation. The overall power conversion efficiency for the P:PCBM:BTD-TNP photovoltaic device is about 1.27%, which has been further enhanced up to 2.6%, when a thermally annealed blend layer is used.

KEYWORDS: low-band-gap small molecule • vinylene copolymer • photovoltaic device • bulk heterojunctions

INTRODUCTION

Solar cells based on organic semiconducting materials are of tremendous interest (1−10) because of their attractive properties such as flexibility, ease of fabrication, and low cost of materials. The most common approach for the fabrication of an efficient conjugated polymer photovoltaic device is to prepare a blend of a conjugated polymer (donor) and a fullerene derivative, such as [6,6]phenyl-C_{61}-butyric acid methyl ester (PCBM) (acceptor) to produce a bulk heterojunction. At present, the power conversion efficiency of photovoltaic devices employing bulk heterojunction active layers is in the range of 5−5.5%, and the highest efficiency of 6.5% has been reported for tandem solar cells (11−18). Photovoltaic devices with optimized performance have been developed using a poly(3-hexylthiophene) (P3HT):PCBM blend and show an ideal incident photon-to-current efficiency (IPCE) in only the mid-wavelength region of visible light. However, the barrier that must be overcome to produce efficient organic photovoltaic devices is to extend the light absorption by the photoactive layer to the longer-wavelength and near-infrared regions, where the maximum photon flux lies, without a reduction in the open-circuit voltage. The overall power conversion efficiency of the organic device depends upon the following factors: the light-harvesting efficiency of the materials in the visible and infrared regions, exciton diffusion to the donor−acceptor interface, photoinduced charge separation, and mobility of the charge carriers produced by photoinduced charge separation (19, 20).

In recent years, significant progress has been made in the synthesis and processing of low-band-gap polymers (21−28), which are capable of absorbing a broad range of solar photons. However, only a few of them have achieved power conversion efficiencies comparable with those of devices fabricated from P3HT (29, 30). A possible route to overcome the low photovoltaic performance observed in a polymer solar cell might be to incorporate a low-band-gap small-molecule donor in the blend with energy levels intermediate to those of polymer and fullerene derivatives (31, 32). Small molecules generally have high mobility and are easily purified and more prone to long-range order than conjugated polymers (33−35).

During selection of the small molecule, it is crucial that the energy levels of the small molecule lie between those of the conjugated polymer and PCBM, in order to avoid the charge trapping in the small molecule. For this purpose, we have used the BTD-TNP small molecule, whose energy levels lie between the copolymer P and PCBM. This molecule

* Corresponding authors. Tel: 91-0291-2720857 (G.D.S.), +30 2610 997115 (J.A.M.). Fax: 91-0291-2720856 (G.D.S.), +30 2610 997118 (J.A.M.). E-mail: sharmagd_in@yahoo.com (G.D.S.), mikroyan@chemistry.upatras.gr (J.A.M.).
Received for review April 8, 2009 and accepted June 29, 2009
[†] JNV University.
[‡] University of Patras.
DOI: 10.1021/am900244y

Published on Web 07/06/2009

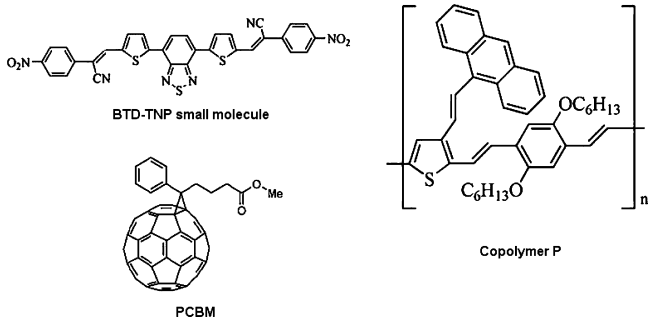

FIGURE 1. Chemical structures of the BTD-TNP small molecule, copolymer P, and PCBM.

absorbs photons in the longer-wavelength region more effectively, whereas the P:PCBM blend has weak absorption. In this paper, we report a comparison of the photovoltaic properties of bulk heterojunction solar cells based on copolymer P:PCBM blends with and without the low-band-gap BTD-TNP small molecule. The short-circuit current (J_{sc}) and the overall power conversion efficiency (η) increase from 2.14 to 5.8 mA/cm^2 and from 0.75 to 1.64%, respectively, when the BTD-TNP molecule has been incorporated in the P:PCBM blend, which has been further enhanced up to 2.6% when a thermally annealed P:PCBM:BTD-TNP blend is used as the active layer in the device. This suggests that the introduction of the low-band-gap small molecules in the donor:acceptor blend improves the light-harvesting properties of the blend, which results in an enhancement in the power conversion efficiency.

EXPERIMENTAL DETAILS

We have used the alternating phenylenevinylene copolymer P containing a side anthracene, which was attached to the thiophene ring via a vinylene bridge as the electron donor and PCBM as the electron acceptor for the present investigation. The chemical structures of conjugated copolymer P, the BTD-TNP small molecule, and PCBM used for this investigation are shown in Figure 1. The synthesis of copolymer P (36) and BTD-TNP (37) and their characterization have been reported elsewhere. The copolymer P is soluble in common organic solvents such as tetrahydrofuran, chloroform, dichloromethane, and toluene owing to the hexyloxy side groups. PCBM was purchased from Aldrich and used as received. Cyclic voltammetry (CV) of copolymer P, BTD-TNP, and PCBM was performed using a potentiostat–galvanostat (PGSTAT-30, Autolab, Eco-Chemie) equipped with three-electrode systems. The three-electrode system was composed of a gold wire, a working electrode, a platinum counter electrode, and a SCE (Ag/Ag^+) reference electrode, calibrated against the ferrocene/ferrocenium (Fc/Fc^+) couple.

The photovoltaic devices have been prepared with a bulk heterojunction active layer of copolymer P:PCBM with and without BTD-TNP, sandwiched between the indium–tin oxide (ITO)-coated glass and the aluminum electrodes. The devices were fabricated on precleaned ITO-coated glass substrates. The copolymer P, PCBM, and BTD-TNP were dissolved in 1,2-dichlorobenzene, separately. The solutions of copolymer P and PCBM and of copolymer P, PCBM, and BTD-TNP were mixed in 1:1 and 1:1:1 ratios to develop the blends of copolymer P:PCBM and copolymer P:PCBM:BTD-TNP, respectively. The thin film blends were spin-coated on ITO-coated glass substrates at 1500 rpm for 2 min. Finally, these blends were transferred to a vacuum chamber, where the aluminum electrode (100 nm)

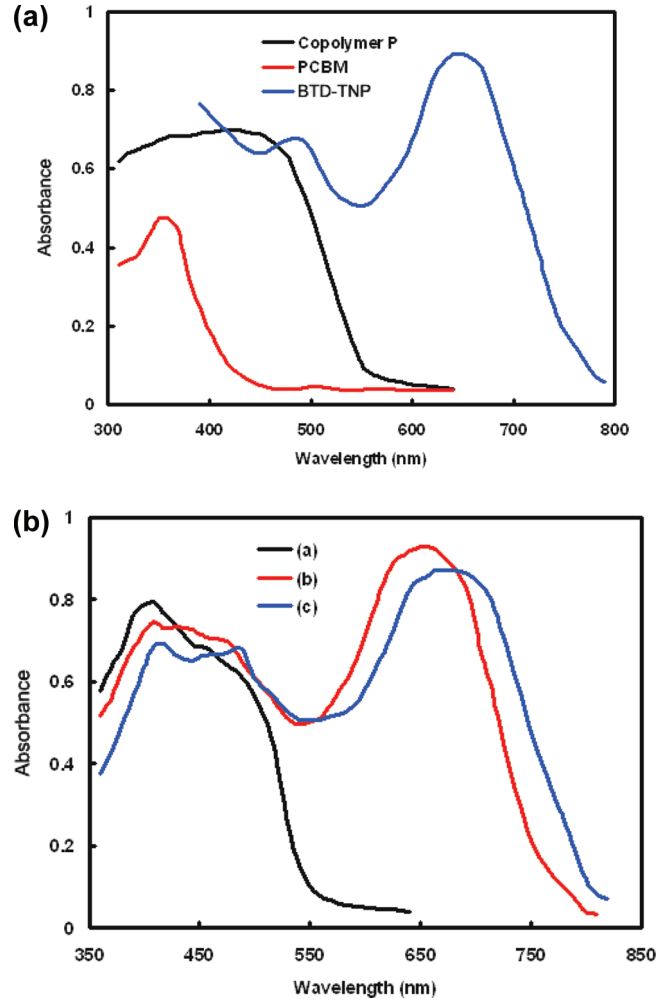

FIGURE 2. (a) Optical absorption spectra of copolymer P, PCBM, and BTD-TNP thin films. (b) Optical absorption spectra of (a) copolymer P:PCBM, (b) copolymer P:PCBM:BTD-TNP, and (c) copolymer P:PCBM:BTD-TNP (annealed) blend thin films.

was deposited by the thermal evaporation method. The active area of the device is about 20 mm^2. For thermal annealing, the blend coated on the ITO substrate was heated at 100 °C for 10 min, before deposition of the aluminum electrode. The current–voltage characteristics of the devices were measured under illumination using a Keithley electrometer with a built-in power supply. The devices were illuminated through the ITO side with a tungsten–halogen lamp at an irradiation intensity of 100 mW/cm^2. The IPCE of the devices was measured by illuminating the device with a tungsten–halogen lamp using a monochromator and measuring the resulting photocurrent with a Keithley electrometer under short-circuit conditions using the following expression:

$$\mathrm{IPCE} = 1240 J_{sc}/\lambda P_{in} \quad (1)$$

where J_{sc} is the short-circuit photocurrent and λ and P_{in} are the wavelength and illumination intensity of the incident light, respectively.

RESULTS AND DISCUSSION

The optical absorption spectra of copolymer P, PCBM, and BTD-TNP thin films are shown in Figure 2a. The thin-film absorption onset of copolymer P is at 534 nm, which

corresponds to an optical absorption band gap (E_g^{opt}) of 2.3 eV. BTD-TNP is a soluble vinylene compound that contains a benzothiadiazole segment and terminal *p*-nitropheyl units. BTD-TNP has an optical band gap of 1.65 eV. The longer-wavelength absorption maximum of BTD-TNP (650 nm) corresponds to the $\pi-\pi^*$ transition of the molecular backbone. The presence of the nitro groups at the terminal phenyls of the BTD-TNP molecule contributes to the broadening of its absorption, as has been well established in the literature (38). The absorption spectrum of BTD-TNP is broad and covers a wide range of the UV−visible and near-infrared spectrum up to 800 nm. This feature is desirable for active materials to be used in organic photovoltaic devices. Therefore, we have used this compound as a low-band-gap small molecule in the present investigation. The optical absorption spectra for bulk heterojunction films comprised of P:PCBM, P:PCBM:BTD-TNP (as cast), and P:PCBM:BTD-TNP (annealed) are also shown in Figure 2b. It seems from this figure that there are broad absorption bands around 390−520 and 620−740 nm in the copolymer P:PCBM:BTD-TNP blend corresponding to copolymer P and BTD-TNP, respectively. The absorption of the blend is a simple superposition of copolymer P and BTD-TNP absorption spectra (as seen in Figure 2a), and there is a small contribution from PCBM in the lower-wavelength region, indicating a homogeneous mixing of components in the blend.

Parts a and b of Figure 3 show the current−voltage characteristics of the devices based on copolymer P:PCBM and P:PCBM:BTD-TNP blends, respectively, under illumination of intensity 100 mW/cm^2. The photovoltaic parameters of these devices are summarized in Table 1. The photovoltaic parameters for the device employing the BTD-TNP:PCBM blend with the same electrodes are also compiled in Table 1 for comparison. The highest power conversion efficiency of the device is about 2.6% for the device based on P:PCBM:BTD-TNP (annealed). The incorporation of BTD-TNP in the blend improves both the short-circuit photocurrent (J_{sc}) and the open-circuit voltage (V_{oc}). However, for the devices based on annealed blends, V_{oc} is slightly decreased. This may be due to the increase in the crystalline nature of the copolymer that results in a decrease of V_{oc} because of the rise in the highest occupied molecular orbital (HOMO) level of the copolymer. The rise in the HOMO level occurs as a result of increased interchain orbital delocalization (39). The increase in J_{sc} with the addition of BTD-TNP is a result of increased absorption at the longer-wavelength region, which is absent in the case of the copolymer P:PCBM blend. The absorption at the longer-wavelength region leads to an increase in exciton generation in BTD-TNP, and the excitons are subsequently dissociated into free charge carriers at the donor:acceptor interfaces formed in the bulk heterojunction active layer.

In order to get information about the origin of the increase in J_{sc} upon the addition of BTD-TNP in the copolymer P:PCBM blend, we have measured the IPCE spectra of the devices. In the case of photovoltaic devices based on blends without BTD-TNP, the IPCE peak is only in the region

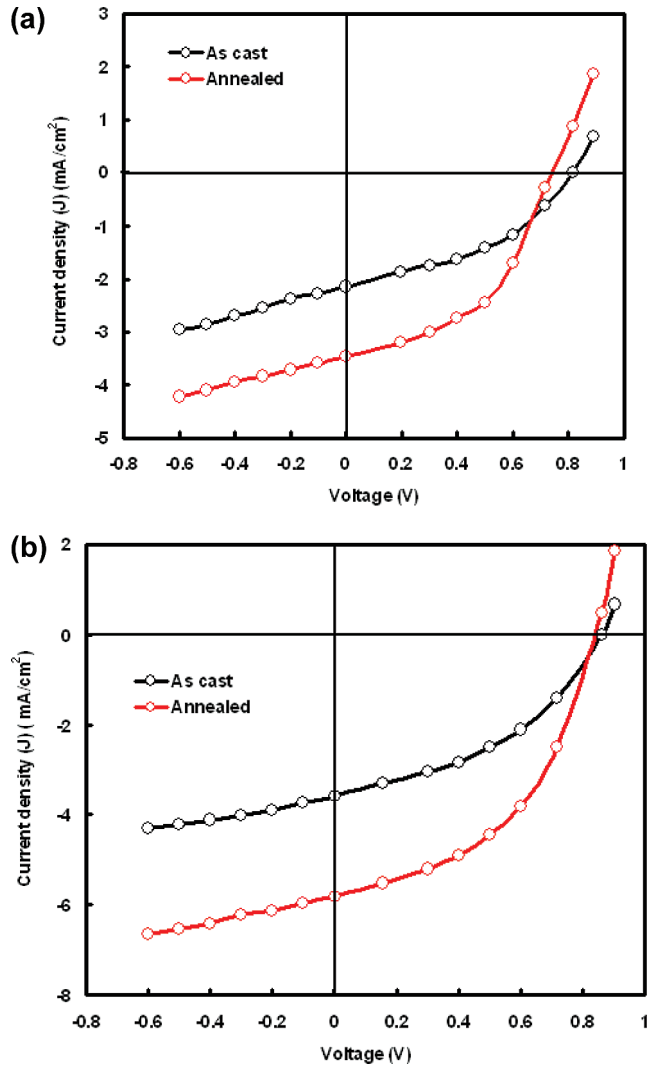

FIGURE 3. (a) Current−voltage characteristics of the devices based on copolymer P:PCBM blends. (b) Current−voltage characteristics of the devices based on copolymer P:PCBM:BTD-TNP blends.

Table 1. Photovoltaic Parameters of the Devices under an Illumination Intensity of 100 mW/cm^2

device	short-circuit current (J_{sc}, mA/cm^2)	open-circuit voltage (V_{oc}, V)	fill factor (FF)	power conversion efficiency (η, %)
ITO/P:PCBM/Al	2.14	0.82	0.43	0.75
ITO/BTD-TNP: PCBM/Al	3.31	0.78	0.47	1.21
ITO/P:PCBM (annealed)/Al	3.4	0.78	0.48	1.27
ITO/P:PCBM:BTD-TNP/Al	3.7	0.85	0.52	1.64
ITO/P:PCBM:BTD-TNP (annealed)/Al	5.8	0.81	0.55	2.6

of 420−550 nm corresponding to the absorption spectrum of the P:PCBM blend. The increase in IPCE of devices with P:PCBM blends upon thermal annealing is attributed to the increase in crystallization of the copolymer. However, the device with P:PCBM:BTD-TNP exhibits two IPCE peaks appearing in the wavelength region of copolymer P absorption and also in the longer-wavelength region of BTD-TNP absorption. Before thermal annealing, the value of IPCE in the region that corresponds to the absorption of copolymer P is comparable to that of the device with copolymer P:PCBM.

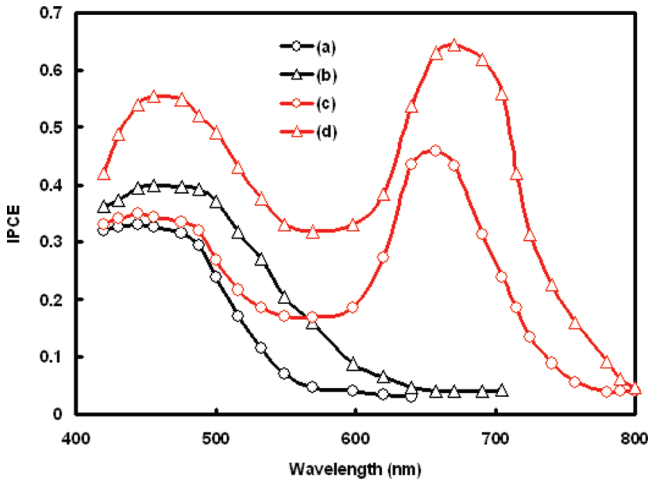

FIGURE 4. IPCE spectra of the photovoltaic devices based on different blends: (a) P:PCBM (as-cast); (b) P:PCBM (annealed); (c) P:PCBM:BTD-TNP (as-cast); (d) P:PCBM:BTD-TNP (annealed).

Table 2. Positions of the LUMO and HOMO Levels of Materials Estimated from CV

material	LUMO (eV)	HOMO (eV)
copolymer P	−2.8	−5.0
PCBM	−4.1	−6.6
BTD-TNP	−3.4	−5.1

This indicates that the photocurrent in this region is due to the generation of excitons due to the absorption of photons by copolymer P and their subsequent dissociation into free charge carriers at the P:PCBM interfaces present in the blend. After thermal annealing, the IPCEs in both absorption bands, which correspond to the copolymer P and BTD-TNP, increase. These phenomena indicate that BTD-TNP is not directly involved in the generation of excitons in the wavelength region, which corresponds to copolymer P absorption. However, BTD-TNP promotes charge separation from the generated excitons in copolymer P.

The HOMO and LUMO levels for copolymer P, BTD-TNP, and PCBM were estimated by CV. For calibration, the redox potential of Fc/Fc^+ was located at 0.09 V to the Ag/Ag^+ electrode. It is assumed that the redox potential of Fc/Fc^+ has an absolute energy level of −4.8 eV relative to the vacuum (40). The energy levels of HOMO and LUMO were then calculated according to the following equations:

$$E_{HOMO} = -(E_{ox} + 4.71)\ \text{eV} \quad \text{and} \quad E_{LUMO} = -(E_{red} + 4.71)\ \text{eV} \tag{2}$$

where E_{ox} and E_{red} are the onset oxidation and reduction potential versus Ag/Ag^+, respectively, observed by CV. The values estimated from CV are listed in Table 2.

Upon the incorporation of BTD-TNP in the P:PCBM blend, BTD-TNP may be located between P and PCBM phases, between PCBM phases, and also between copolymer P phases. The energy level diagram of the copolymer P, BTD-TNP, and PCBM is shown in Figure 5. As shown in Figure 5a, the exciton generated in BTD-TNP, when BTD-TNP is

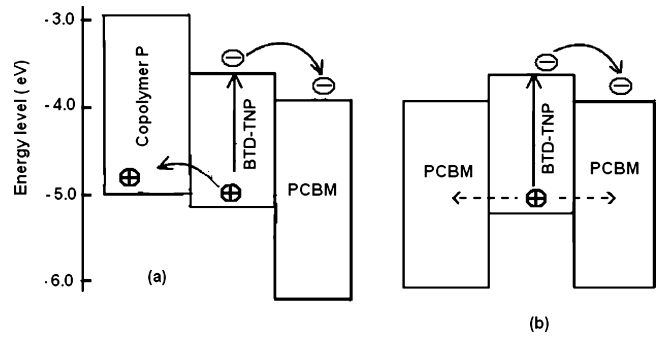

FIGURE 5. Energy level diagram of BTD-TNP and surrounding materials: (a) BTD-TNP located at the interface between copolymer P and PCBM; (b) BTD-TNP located in the PCBM domain.

located between P and PCBM, injects an electron into PCBM and a hole into copolymer P because the HOMO level of BTD-TNP is lower than the HOMO level of copolymer P. This forms a favorable energy cascade in both the LUMO and HOMO levels of the materials used in the device. This energetic cascade is essential for the bulk heterojunction for efficient photoinduced charge transfer. However, when BTD-TNP is located at the PCBM domain, BTD-TNP can only inject the electron into the PCBM domain but cannot inject a hole into the surrounding PCBM domain because of the lower HOMO level of PCBM. Similarly, when BTD-TNP is located at the copolymer P domain, the same situation is true. Therefore, only the BTD-TNP molecule, which is located near the interface of P:PCBM, can contribute to the photocurrent generation.

The photocurrent originating from the BTD-TNP addition in the P:PCBM blend indicates that some of the BTD-TNP molecules are located at the copolymer P:PCBM interface even before thermal annealing of the blend. As the IPCE at 650 nm increases from 0.45 to 0.64, when the thermally annealed blend is used in the device, the absorption spectra of the blend remain the same. This may be due to the enhanced charge collection efficiency, which is improved by the formation of an interpenetrating network, upon thermal annealing. In addition to that, it may be possible that a number of BTD-TNP molecules located at the P-PCBM interface increase upon thermal annealing because of the increased crystallinity of the conjugated copolymer and aggregation of the nanocrystalline PCBM domain. When the blend is thermally annealed, the BTD-TNP molecules located in the copolymer P or PCBM domain may be expelled from each domain into the interface by crystallization of the conjugated copolymer P and aggregation of the nanocrystalline PCBM domain.

As mentioned earlier, there are two mechanisms responsible for the increase in J_{sc} by the addition of BTD-TNP molecules in the copolymer P:PCBM blend. One is that additional absorption at the longer-wavelength region by the BTD-TNP molecule directly contributes to the increase in J_{sc}. In addition to the above mechanism, the BTD-TNP molecules that are located at the copolymer P:PCBM interface promote the charge separation for generated excitons in copolymer P at the wavelength region of 440−570 nm. The combined

effect of the above two mechanisms improves the overall power conversion efficiency.

CONCLUSION

In conclusion, we have shown that the addition of the BTD-TNP small molecule in the copolymer P:PCBM bulk heterojunction solar cell improves the photocurrent and power conversion efficiencies. The broader absorption of BTD-TNP molecules at the longer-wavelength region effectively harvests photons in this region. Moreover, the allocation of BTD-TNP molecules at the copolymer P:PCBM interface contributes to the enhancement in the power conversion efficiency. In the wavelength region of 440−520 nm, the BTD-TNP molecules that are located between copolymer P and PCBM contribute to the photocurrent. The BTD-TNP molecules that are located at the P:PCBM interface contribute also to the photocurrent through the effective dissociation of the generated excitons in the copolymer phase at the shorter-wavelength region. A further improvement in the power conversion efficiency of the device based on the thermally annealed blend is attributed to the increase in the number of BTD-TNP molecules at the copolymer P/PCBM interface due to crystallization of the conjugated copolymer P.

Acknowledgment. G.D.S., P.S., and P.B. greatly acknowledge the financial support from the Department of Science and Technology, Government of India, New Delhi, India, and the Council for Scientific and Industrial Research, Government of India. We are also thankful to Dr. M. S. Roy, Scientist, Defence Laboratory, Jodhpur, India, for providing the CV measurement facility.

Supporting Information Available: The synthesis and characterization of BTD-TNP small molecule and copolymer P. This material is available free of charge via the Internet at http://pubs.acs.org.

REFERENCES AND NOTES

(1) Sariciftci, N. S.; Smilowitz, L.; Heeger, A. J.; Wudl, F. *Science* **1992**, *258*, 1474–1476.
(2) Kim, J. Y.; Lee, K.; Coates, N. E.; Moses, D.; Nguyen, T. Q.; Dante, M.; Heeger, A. J. *Science* **2007**, *317*, 222–225.
(3) Kinoshita, Y.; Hasobe, T.; Murata, H. *Appl. Phys. Lett.* **2007**, *91*, 083518/1–083518/3.
(4) Zhang, C. F.; Tong, S. W.; Jiang, C. Y.; Kang, E. T.; Chan, D. S. H.; Zhu, C. X. *Appl. Phys. Lett.* **2008**, *93*, 043307/1–043307/3.
(5) Chan, M. Y.; Lai, S. L.; Fung, M. K.; Lee, C. S.; Lee, S. T. *Appl. Phys. Lett.* **2007**, *90*, 023504/1–023504/3.
(6) Dai, J. G.; Jiang, X. X.; Wang, H. B.; Yan, D. H. *Appl. Phys. Lett.* **2007**, *91*, 253503/1–253503/3.
(7) Colladet, K.; Fourier, S.; Cleij, T. J.; Lutsen, L.; Gelan, J.; Vanderzande, D.; Nguyen, L. H.; Neugebauer, H.; Sariciftci, N. S.; Aguirre, A.; Janssen, G.; Goovaerts, E. *Macromolecules* **2007**, *40*, 65–72.
(8) Zhang, C.; Tong, S. W.; Zhu, C.; Jiang, C.; Kang, E. T.; Chan, D. S. H. *Appl. Phys. Lett.* **2009**, *94*, 103305/1–103305/3.
(9) Mei, J.; Ogawa, K.; Kim, Y. G.; Heston, N. C.; Arenas, D. J.; Nasrollahi, Z.; McCarley, T. D.; Tanner, D. B.; Reynolds, J. R.; Schanze, K. S. *ACS Appl. Mater. Interfaces* **2009**, *1*, 150–161.
(10) Scharber, M. C.; Wuhlbacher, D.; Koppe, M.; Denk, P.; Waldauf, C.; Heeger, A. J.; Brabec, C. L. *Adv. Mater.* **2006**, *18*, 789–794.
(11) Thompson, B. C.; Frechet, J. M. J. *Angew. Chem., Int. Ed.* **2008**, *47*, 58–77.
(12) Reyes-Reyes, M.; Kim, K.; Carroll, D. L. *Appl. Phys. Lett.* **2005**, *87*, 083506/1–083506/3.
(13) Li, G.; Shrotriya, V.; Huang, J. S.; Yao, Y.; Moriarty, T.; Emery, K.; Yang, Y. *Nat. Mater.* **2005**, *4*, 864–868.
(14) Kim, Y.; Cook, S.; Tuladhar, S. M.; Choulis, S. A.; Nelson, J.; Durrant, J. R.; Bradley, D. D. C.; Giles, M.; Mcculloch, I.; Ha, C. S.; Ree, M. *Nat. Mater.* **2006**, *5*, 197–203.
(15) Kim, J. Y.; Kim, S. H.; Lee, H. H.; Lee, K.; Ma, W. L.; Gong, X.; Heeger, A. J. *Adv. Mater.* **2006**, *18*, 572–576.
(16) Kim, K.; Liu, J.; Namboothiry, M. A. G.; Carroll, D. L. *Appl. Phys. Lett.* **2007**, *90*, 163511/1–163511/3.
(17) Kim, J. Y.; Lee, K.; Coates, N. E.; Moses, D.; Nguyen, T. Q.; Dante, M.; Heeger, A. J. *Science* **2007**, *317*, 222–225.
(18) Green, M. A.; Emery, K.; Hishikawa, Y.; Warta, W. *Prog. Photovoltaics* **2008**, *16*, 435–440.
(19) Brabec, C. J.; Sariciftci, N. S.; Hummelen, J. C. *Adv. Funct. Mater.* **2001**, *11*, 15–26.
(20) Chen, L. M.; Hong, Z.; Li, G.; Yang, Y. *Adv. Mater.* **2009**, *21*, 1434–1449.
(21) Wang, X. Z.; Wong, W. Y.; Cheung, K. Y.; Fung, M. K.; Djurisic, A. B.; Chan, W. K. *Dalton Trans.* **2008**, 5484–5494.
(22) Liu, L.; Ho, C. L.; Wong, W. Y.; Cheung, K. Y.; Fung, M. K.; Lam, W. T.; Djurisic, A. B.; Chan, W. K. *Adv. Funct. Mater.* **2008**, *18*, 2824–2833.
(23) Wong, W. Y.; Wang, X. Z.; He, Z.; Chan, K. K.; Djusisic, A. B.; Cheung, K. Y.; Yip, C. T.; Ng, A. M. C.; Xi, Y. Y.; Mak, C. S. K.; Chan, W. K. *J. Am. Chem. Soc.* **2007**, *129*, 14372–14380.
(24) Chen, C. P.; Chain, S. H.; Chao, T. C.; Ting, C.; Ko, B. T. *J. Am. Chem. Soc.* **2008**, *130*, 12828–12833.
(25) Blouin, N.; Michaud, A.; Gendron, D.; Wakim, S.; Blair, E.; Neagu-plesu, R.; Belletete, M.; Durocher, G.; Tao, Y.; Leclerc, M. *J. Am. Chem. Soc.* **2008**, *130*, 732–734.
(26) Liang, Y.; Wu, Y.; Feng, D.; Tsai, S. T.; Son, H. J.; Li, G.; Yu, L. *J. Am. Chem. Soc.* **2009**, *131*, 56–57.
(27) Wong, W. Y. *Macromol. Chem. Phys.* **2008**, *209*, 14–24.
(28) Wong, W. Y.; Wang, X. Z.; He, Z.; Djurisic, A. B.; Yip, C. T.; Cheung, K. Y.; Wang, H.; Mak, C. S. K.; Chan, W. K. *Nat. Mater.* **2007**, *6*, 521–527.
(29) Peet, J.; Kim, J. Y.; Coates, N. E.; Ma, W. L.; Moses, D.; Heeger, A. J.; Bazan, G. C. *Nat. Mater.* **2007**, *6*, 497–500.
(30) Wienk, M. M.; Turbiez, M.; Gilot, J.; Janssen, R. A. *Adv. Mater.* **2008**, *20*, 2556–2560.
(31) Belcher, W. J.; Wagner, K. I.; Dastoor, P. C. *Sol. Energy Mater. Sol. Cells* **2007**, *91*, 447–452.
(32) Ltaief, A.; Chaabane, R. B.; Bouazizi, A.; Davenas, J. *Mater. Sci. Eng., C* **2006**, *26*, 344–347.
(33) Tamayo, A. B.; Walker, B.; Nguyen, T.-Q. *J. Phys. Chem. C* **2008**, *112*, 11545–11551.
(34) Lloyd, M. T.; Mayer, A. C.; Subramanian, S.; Mourney, D. A.; Herman, D. J.; Bapat, A.; Anthony, J. E.; Malliaras, G. G. *J. Am. Chem. Soc.* **2007**, *129*, 9144–9149.
(35) Roquet, S.; Cravino, A.; Leriche, P.; Aleveque, O.; Frere, P.; Roncali, J. *J. Am. Chem. Soc.* **2006**, *128*, 3459–3466.
(36) Mikroyannidis, J. A.; Stylianakis, M. M.; Suresh, P.; Sharma, G. D. *Sol. Energy Mater. Sol. Cells* **2009**, accepted for publication.
(37) Mikroyannidis, J. A.; Stylianakis, M. M.; Suresh, P.; Balraju, P.; Sharma, G. D. **2009**, submitted for publication.
(38) He, Y.; Wang, X.; Zhang, J.; Li, Y. *Macromol. Rapid Commun.* **2009**, *30*, 45–51.
(39) Vandewal, K.; Gadisa, A.; Oosterbaan, W. D.; Mance, J. V. *Adv. Funct. Mater.* **2008**, *18*, 2064–2070.
(40) Pommerehne, J.; Vestewber, H.; Guss, W.; Mahrt, R. F.; Bassler, H.; Porsch, M.; Daub, J. *Adv. Mater.* **1995**, *7*, 551–554.

AM900244Y